Journal of Traditional and Complementary Medicine 13 (2023) 193–206

Contents lists available at ScienceDirect

Journal of Traditional and Complementary Medicine

journal homepage: http://www.elsevier.com/locate/jtcme

Cell-free *Lactiplantibacillus plantarum* OC01 supernatant suppresses IL-6-induced proliferation and invasion of human colorectal cancer cells: Effect on β-Catenin degradation and induction of autophagy

Letizia Vallino [a, 1], Beatrice Garavaglia [a, 1], Annalisa Visciglia [b], Angela Amoruso [b], Marco Pane [b], Alessandra Ferraresi [a], Ciro Isidoro [a, *]

[a] Laboratory of Molecular Pathology, Department of Health Sciences, Università del Piemonte Orientale "A. Avogadro", Via P. Solaroli 17, 28100, Novara, Italy
[b] Probiotical Research Srl, via E. Mattei, 3, 28100, Novara, Italy

ARTICLE INFO

Article history:
Received 20 January 2023
Received in revised form
13 February 2023
Accepted 16 February 2023
Available online 21 February 2023

Keywords:
Probiotics
Microbiota
Colorectal cancer
Inflammation
Butyrate
β-Catenin
Autophagy
Cell proliferation
Cell migration

ABSTRACT

Background and aim: Gut microbiota is considered as a complex organ of human body. The interaction between the host and microbiota is dynamic and controlled by a huge number of factors, such as lifestyle, geography, pharmaceuticals, diet, and stress. The breakdown of this relationship could change microbiota composition favoring the onset of several diseases, including cancer. Metabolites released by microbiota bacterial strains have been reported to elicit protective effects on the mucosa that could contrast cancer development and progression. Here, we tested the ability of specific probiotic strain *Lactiplantibacillus plantarum* OC01-derived metabolites (NCIMB 30624) to contrast the malignant features of colorectal cancer (CRC) cells.

Experimental procedure: The study was performed on two cell lines, HCT116 and HT29, cultured in 2D and 3D, and focused on the hallmarks of cell proliferation and migration.

Results and conclusion: Probiotic metabolites reduced cell proliferation both in 2D and 3D-spheroid cultures, the latter model mimicking the growth *in vivo*. The bacterial metabolites also contrasted the pro-growth and pro-migratory activity of inteurleukin-6 (IL-6), an inflammatory cytokine abundantly found in the tumor microenvironment of CRC. These effects were associated with inhibition of the ERK and of the mTOR/p70S6k pathways and with the inhibition of the E−to N-Cadherin switch. In a parallel study, we found that sodium butyrate (a representative of the main probiotic metabolites) induced autophagy and β-Catenin degradation, which is consistent with the growth inhibitory activity. The present data indicate that the metabolites of *Lactiplantibacillus plantarum* OC01 (NCIMB 30624) elicits anti-tumor effect and support its possible inclusion as adjuvant therapy of CRC for limiting cancer growth and progression.

1. Introduction

Intestinal microbes, represented by bacteria, virus, and fungi, create a tight crosstalk with the host, regulating health, physiology, metabolism, immune system, and preventing pathogens colonization. The gut microbiota plays an essential role in maintaining intestinal function and homeostasis.[1] As a result of fiber fermentation, commensal bacteria, being *Bacteroidetes* and *Firmicutes* the predominant *phyla*, produce short chain fatty acids (SCFAs), with butyrate being the most relevant one, that are exploited by intestinal colonocytes as energy source for gut cell proliferation and differentiation.[2,3]

Abbreviations: CRC, Colorectal cancer; IL-6, interleukin-6; NaB, sodium butyrate; SCFAs, short chain fatty acids; EMT, epithelial to mesenchymal transition; CFS, cell-free supernatant.

* Corresponding author. Dipartimento di Scienze della Salute, Università del Piemonte Orientale "A. Avogadro", Via P. Solaroli 17, 28100, Novara, Italy.
E-mail addresses: letizia.vallino@uniupo.it (L. Vallino), beatrice.garavaglia@uniupo.it (B. Garavaglia), a.visciglia@probiotical.com (A. Visciglia), a.amoruso@probiotical.com (A. Amoruso), m.pane@probiotical.com (M. Pane), alessandra.ferraresi@med.uniupo.it (A. Ferraresi), ciro.isidoro@med.uniupo.it (C. Isidoro).

Peer review under responsibility of The Center for Food and Biomolecules, National Taiwan University.

[1] These authors equally contributed.

https://doi.org/10.1016/j.jtcme.2023.02.001

Pathogenic changes in the function and composition of gut microbiota, defined as dysbiosis, are associated with several diseases, including chronic inflammation of the intestine and colorectal cancer (CRC).[4–6] CRC is one of the most prevalent and deadly cancer worldwide. Protocol management of CRC patients at early stages includes surgery resection followed by chemotherapy (e.g., 5-fluorouracil and leucovorin in combination with oxaliplatin or irinotecan), and target therapy with monoclonal antibodies or peptides targeting VEGF or EGFR.[7,8] Unfortunately, the effectiveness of current anticancer treatment is limited because of the presence of diffused metastases at diagnosis.[9,10] Clinical and experimental evidence underscores the role of the inflammatory tumor microenvironment in the development and progression of CRC.[11] In this context, IL-6 released by cancer cells and stromal cells (mainly cancer-associated fibroblasts) is considered the main culprit. *In vitro*, IL-6 was shown to promote anchorage-independent growth and migration of CRC cells.[12] Consistently, the serum levels of IL-6 were found much higher in CRC patients than in healthy controls, and were associated with increased tumor growth and aggressiveness, metastases, and bad clinical outcome.[13–15]

In this context, it has been shown that a reciprocal influence exists between the intestinal inflammatory status and the microbiota that eventually impacts on CRC development and progression.[16]

Probiotics and their metabolites positively affect the composition of gut microbiota (qualitatively and quantitatively), and also modulate metabolic activity, by enhancing the integrity of intestinal epithelial barrier, increasing the accumulation of antioxidants and anti-carcinogenic metabolites against CRC, reducing intestinal inflammation state (e.g., IL-6, IL-8, TNF-α), and protecting from carcinogenesis.[17–19]

Here, we tested the efficacy of cell-free *Lactiplantibacillus plantarum* OC01 (NCIMB 30624) supernatant in suppressing the growth and migration of CRC cells induced by IL-6 in two human CRC cell lines (namely HCT116 and HT-29) differing for their genetic background and propensity to grow and to migrate. We found that probiotic metabolites contrast the growth of CRC cells cultured as 2D or 3D spheroids as well as their migration and invasion through the transwell. In a parallel study conducted in HCT116 cells (which bear a mutation in β-Catenin gene), we found that butyrate, a SCFA released by probiotic strain, induced the autophagy-mediated degradation of β-Catenin, thus preventing the transcription of genes necessary for cell cycle progression. Of note, this probiotic strain contrasted the pro-growth and pro-migratory effects of IL-6, thus supporting the view that supplementation of certain gut probiotic strains may represent a potential strategy as adjuvant therapeutics to limit cancer malignancy.

2. Materials and methods

2.1. Cell culture

Human colorectal cancer cell lines HCT116 (CCL-247™) and HT29 (HTB-38™) with different genetic background (Table 1) were purchased from the American Type Culture Collection (ATCC) (Manassas, Virginia, USA). The cell lines were cultured in Dulbecco's Modified Eagle Medium (DMEM, cod. D5671; Sigma-Aldrich, St. Louis, MO), supplemented with 10% heat-inactivated fetal bovine serum (FBS, cod. ECS0180L; Euroclone, Milan, Italy), 1% glutamine (cod. G7513; Sigma-Aldrich, St. Louis, MO, USA), and 1% penicillin/streptomycin (PES, cod. P0781; Sigma-Aldrich, St. Louis, MO, USA). Human fibroblasts were cultured in RPMI-1640 (cod. R8758; Sigma-Aldrich, St. Louis, MO, USA) supplemented as described above. All the cell lines were cultured under standard conditions (37 °C, 95 v/v% air: 5 v/v% CO_2).

2.2. Probiotic formulation and treatments

Lactiplantibacillus plantarum OC01 (NCIMB 30624) from the Probiotical SpA collection has been used in the present study; the probiotic strain was stored in 20% glycerol at −80 °C. More than 90% of the cells were alive upon thawing. Before use, microorganisms were grown in anaerobic conditions with CO_2-generating kits (Anaerocult A; Merck, Darmstadt, Germany) overnight at 37 °C in de Man-Rogosa-Sharpe (MRS) broth containing 0.05% cysteine hydrochloride, and then sub-cultured over the mid-log phase. For the enumeration of live bacteria, the BD Cell Viability Kit (BD Biosciences, Milan, Italy) was used as instructed by the manufacturer.

For stimulation experiments, eukaryotic cell cultures were exposed to the supernatants of overgrown probiotic strain of interest. Cell-free supernatant of OC01 contained all the catabolic and anabolic products released by 10 billion viable probiotic cells during overnight overgrowth, and it was used after filtration with a 0.2 μm filter-syringe to remove all viable cells.

Cell cultures were supplemented with different doses (10 μl, 100 μl, and 200 μl) of the cell-free supernatant of OC01 in 1 ml of final volume of DMEM medium. The 10 μl dose was shown effective and non-toxic and was used throughout all the experiments. Untreated cells were exposed to DMEM culture medium. The control MRS broth at 10 μl/ml in DMEM was ineffective.

Additional treatments included 50 ng/ml IL-6 (cod. 11340066; Immunotools, Friesoythe, Germany) and 1 mM sodium butyrate (NaB, cod. B5887; Sigma-Aldrich, St. Louis, MO, USA), dissolved in sterile water.

2.3. Cell counting and cell cycle analysis

Cells were plated in p35 Petri dishes at the density of 50,000 cell/cm^2. The following day, cells were counted (time 0) and then treated as indicated for 24, 48, and 72 h. At the end of each experimental time-point, cells were trypsinized and collected, and cell suspension was diluted 1:1 with Trypan Blue (cod. T8154; Sigma-Aldrich, St. Louis, MO, USA). Cell counting was performed in triplicates for each experimental condition. For cell cycle analysis, cells were fixed in 70% ice-cold ethanol and stored at −20 °C. Before starting the cytofluorimetric analysis, RNAse (50 μg/ml) was added to cells for 30 min at 37 °C. Cells were stained with propidium iodide (PI, 50 μg/ml; cod. P4170; Sigma-Aldrich, St. Louis, MO, USA) and acquired by using FacScan flow cytometer (FACSCalibur, Becton Dickinson, Eysins, Switzerland). The processing of the data obtained was performed using the free tool Flowing Software 2.5.1 (Turku Center for Biotechnology, University of Turku, Finland).

Table 1
Mutational status of relevant oncogenes and tumor suppressor genes in colorectal cancer cell lines. HCT116 were isolated from the large intestine of colorectal cancer-affected adult male. HT29 was isolated from a primary tumor obtained from a white, female patient with colorectal adenocarcinoma (*APC*, Adenomatous Polyposis Coli; *CTNNB1*, β-Catenin gene).

	KRAS	TP53	APC	CTNNB1
HCT116	G13D (Missense)	Wild-type	Wild-type	S45del
HT29	Wild-type	R273H	E853*(Nonsense): T1556Nfs*3(Insertion-Frameshift)	NA

2.4. Antibodies

The following primary antibodies (at the dilution indicated) were used for either immunofluorescence or Western blotting: mouse *anti*-p21 (1:100, cod. B1313; Santa Cruz, Biotechnology, Dallas, TX, USA); rabbit *anti*-Ki67 (1:100, cod. HPA001164; Sigma-Aldrich, St. Louis, MO, USA); rabbit *anti*-phospho-ERK1/2 (Thr202/Tyr204, Thr185/Tyr187) (1:500, cod. 05–797R; Millipore, Burlington, MA, USA); mouse *anti*-ERK1/2 (1:500, cod. 05–1152; Millipore, Burlington, MA, USA); rabbit *anti*-phospho-S6 (Ser235/236) (1:500, cod. 4856; Cell Signaling, Danvers, MA, USA); rabbit *anti*-S6 (1:500, cod. 2217; Cell Signaling, Danvers, MA, USA); mouse *anti*-N-Cadherin (1:50, cod. 610920; BD Biosciences, Franklin Lakes, NJ); mouse *anti*-E-Cadherin (1:50, cod. 610404; BD Biosciences, Franklin Lakes, NJ); rabbit *anti*-LC3 (1:1000, cod. L7543; Sigma-Aldrich, St. Louis, MO, USA); mouse anti-LAMP1 (1:1000, cod. 555798; BD, Biosciences, Franklin Lakes, NJ); rabbit anti- β-Catenin (1:500, cod. PA5-77934; Invitrogen, Paisley, UK); mouse *anti*-β-Actin (1:2000, cod. A5441; Sigma-Aldrich, St. Louis, MO, USA); mouse *anti*-β-Tubulin (1:1000, cod. T5326; Sigma-Aldrich, St. Louis, MO, USA); rabbit *anti*-GAPDH (1:1000, cod. G9545; Sigma-Aldrich, St. Louis, MO, USA).

2.5. Immunofluorescence

Cells were seeded onto sterile coverslips at the density of 25,000 - 30,000 cells/cm^2, left to adhere, and treated as reported. At the end of the experiment, the coverslips were fixed within ice-cold methanol, permeabilized with 0.2% Triton-PBS, and incubated overnight at 4 °C with specific primary antibodies dissolved in 0.1% Triton-PBS +10% FBS. The following day, coverslips were incubated for 1 h at room temperature with secondary antibodies (diluted in 0.1% Triton-PBS + 10% FBS), followed by AlexaFluor488-conjugated goat-anti rabbit IgG (1:000, cod. A32731; Invitrogen, Paisley, UK) or AlexaFluor555-conjugated goat-anti mouse IgG (1:1000, cod. A32727; Invitrogen, Paisley, UK), as appropriate. Nuclei were stained with UV fluorescent dye DAPI (40,6-diamidino-2-phenylindole). Coverslips were mounted onto glass using SlowFade reagent (cod. S36936; Life Technologies, Paisley, UK) and imaged with a fluorescence microscope (Leica Microsystems DMI6000; Wetzlar, Germany). Fluorescence intensity was measured using the ImageJ software.

2.6. 3D-spheroid forming assay

3D spheroids were obtained by culturing the cells in non-adherent conditions using polyhema-covered plates.[20] Poly(2-hydroxyethylmethacrylate) or polyhema (cod. P3932; Sigma-Aldrich, St. Louis, MO, USA) was dissolved in 95% ethanol and left under rotation overnight at 50 °C. The stock solution was diluted in ethanol to obtain a working solution of 120 mg/ml. P35 Petri dishes were coated with this solution and left to completely dry under the biological hood, and then stored at room temperature until use. Cells were seeded at the density of 500,000 (for homogenates) or 250,000 cells (for immunofluorescence) per plate and treated according to the experimental conditions. The growth of spheroids was monitored by taking pictures at phase contrast microscope (Zeiss, Oberkochen, Germany; AXIOVERT 40CFL, magnification 5 ×) at each time point. The quantification of the dimension of the spheroids was performed with ImageJ software 1.51 (National Institutes of Health, MD, USA).

To assess cell proliferation in 3D spheroids, we employed the plasma membrane staining with a vital fluorescent dye that undergoes dilution along with cell division.[20] Cell lines were stained with 1 μM DiD (cod. V22887; Life Technologies, Paisley, UK) in serum-free medium at 37 °C for 30 min, then dissolved in complete medium, plated as described above for 3D spheroids and treated as indicated. At day 0 and day 7 the spheroids were cytospotted on glass slides. The intensity of DiD retention was immediately acquired at the fluorescence microscope (Leica Microsystems, Wetzlar, Germany; DMI6000) and then quantified with the software ImageJ. Three-dimensional immunofluorescence was performed on spheroids cytospotted on glass slides at day 7. Spheroids were fixed in methanol, permeabilized for 30 min in 0.5% Triton-PBS, and processed as described previously.[21]

2.7. Western blotting analysis

Cells were seeded in Petri dishes at the density of 35,000–40,000 cells/cm^2 and treated as indicated when confluence reached approximately 80%. Cell homogenates were prepared by freeze-thawing and ultrasonication in RIPA lysis buffer containing protease inhibitors as described in Ref. 21. The blots were detected using enhanced chemiluminescence reagents (ECL, cod. NEL105001EA; PerkinElmer, Waltham, MA) and developed with the ChemiDoc XRS instrument (BioRad, Hercules, CA, USA). Intensity of the bands was estimated by densitometry using Image Lab 6.0 (BioRad, Hercules, CA, USA).

2.8. Wound healing migration assay

Cells were seeded in p35 Petri dishes at the density of 60,000–50,000 cells/cm^2 and cultured until confluence. The cell monolayer was scratched with a sterile yellow pipette tip to produce a straight line and the debris washed out with PBS.[22] To prevent starvation-induced autophagy, medium and treatments were renovated every 24 h. The open gap was photographed with a camera at phase contrast microscope (magnification 5X, Zeiss AXIOVERT 40CFL, Zeiss, Oberkochen, Germany) at the indicated times. The rate of healing was estimated by ImageJ software based on the area free of cells as previously reported.[22] Data are calculated for three different fields per each condition.

2.9. Transwell migration assay

Cells were seeded in Petri dishes at the density of 50,000 cells/cm^2 and cultured until reaching 80% of confluence. Medium and treatments were renewed every day. After 48 h of culture, cells were trypsinized, collected, and counted. An aliquot of 50,000 cells per experimental condition was resuspended in serum-free medium supplemented as indicated per the treatment and plated in uncoated inserts (Transwell® Permeable Supports, Polycarbonate (PC) Membrane; 6.5 mm Insert; 8.0 μm pore size Polycarbonate Membrane; cod. 3422, Corning Incorporated Costar, NY, USA). Each insert was placed in a 24-well plate containing complete media and the plate was placed in the incubator. After 24 h of incubation, a different fraction of each cell population had migrated through the porous membrane to the underside of the inserts. The migrated cells were washed in PBS, fixed in methanol for 30 min to allow cell fixation, washed in PBS, and then stained for 1 h with eosin-hematoxylin solution (cod. 05-M06002; Bio-Optica, Milan, Italy). The inserts were washed in PBS and let dry for at least 1 day. Inserts were cut and mounted onto slides using Biomount reagent (cod. 05-BMHM100, Bio-Optica, Milan, Italy) and photographed in random fields at bright-field microscope (magnification 20X; Panoramic Midi, Sysmex, Bornbarch, Germany).[21] The amount of migrated cells (as mirrored by the staining intensity) was estimated by ImageJ software. Data are calculated as average of different fields per each condition.

A

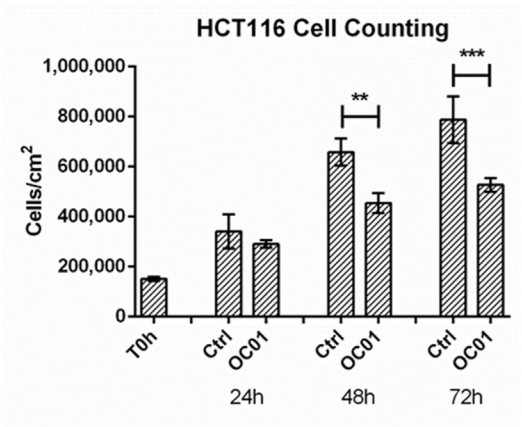

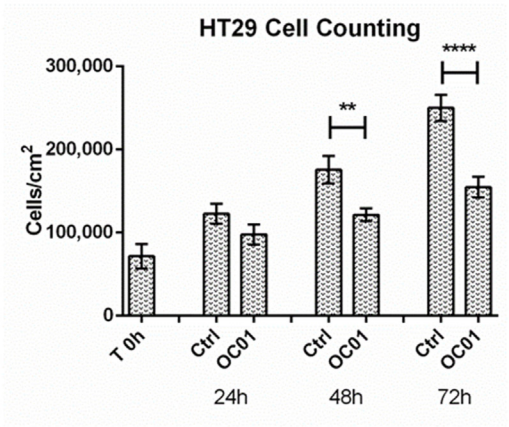

B

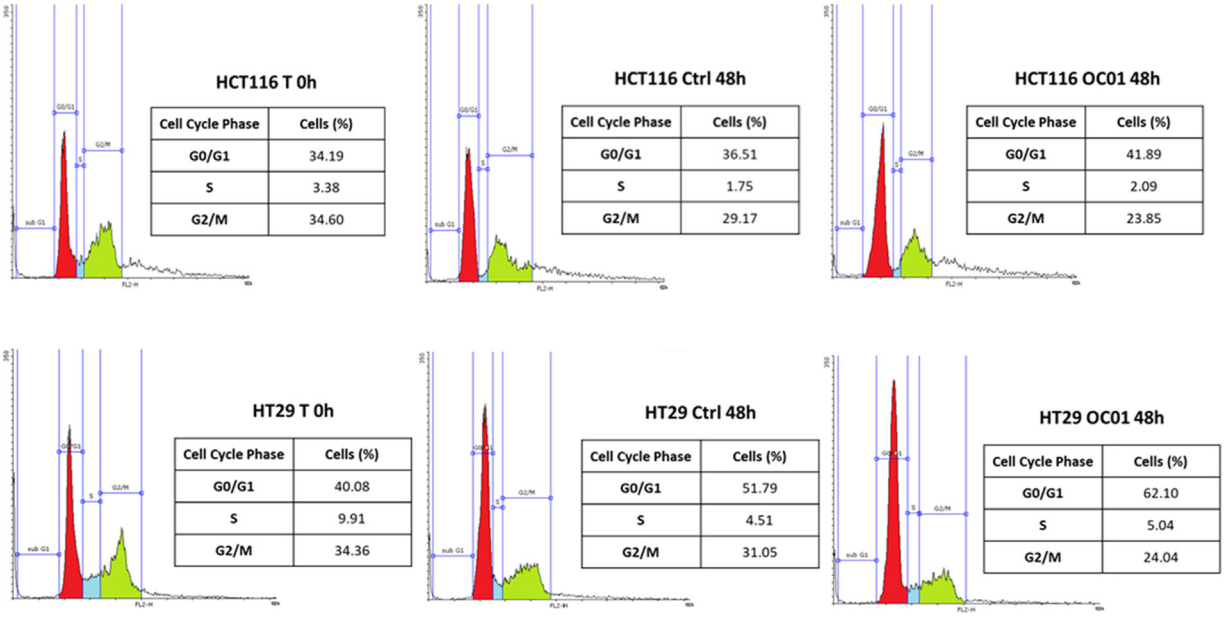

HCT116 T 0h

Cell Cycle Phase	Cells (%)
G0/G1	34.19
S	3.38
G2/M	34.60

HCT116 Ctrl 48h

Cell Cycle Phase	Cells (%)
G0/G1	36.51
S	1.75
G2/M	29.17

HCT116 OC01 48h

Cell Cycle Phase	Cells (%)
G0/G1	41.89
S	2.09
G2/M	23.85

HT29 T 0h

Cell Cycle Phase	Cells (%)
G0/G1	40.08
S	9.91
G2/M	34.36

HT29 Ctrl 48h

Cell Cycle Phase	Cells (%)
G0/G1	51.79
S	4.51
G2/M	31.05

HT29 OC01 48h

Cell Cycle Phase	Cells (%)
G0/G1	62.10
S	5.04
G2/M	24.04

C

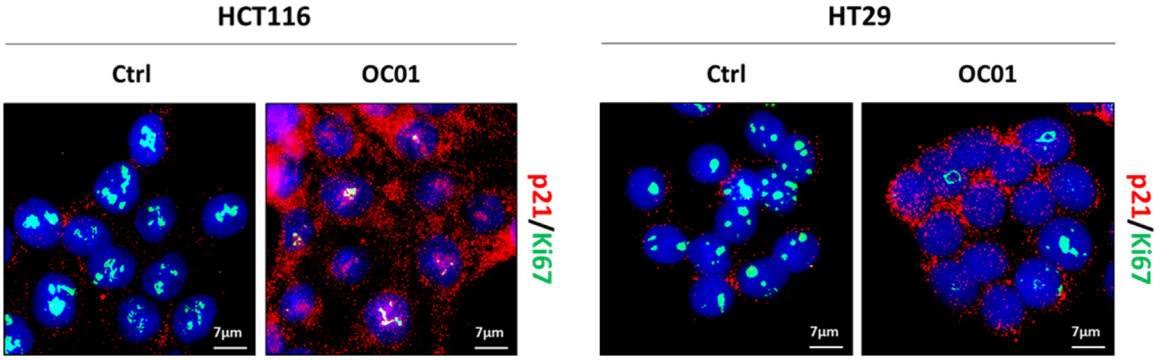

Fig. 1. Cell-free OC01 supernatant reduces colorectal cancer (CRC) cell proliferation. HCT116 and HT29 cell lines were plated and treated with cell-free OC01 supernatant. Medium was replaced, and treatment re-added at 24 h. **A)** Cell counting was performed up to 72-h treatment in triplicates per each experimental condition. The graph represents the average ± SD (significance was considered as follow: ****p < 0.0001; ***p < 0.001; **p < 0.01). **B)** The panel reports the cytofluorimetric analysis of the cell cycle performed at 48-h treatment in triplicates per each experimental condition and quantified by using FacScan flow cytometer. The area under each peak shows a different fraction of cell population in the respective cell cycle phase. **C)** After 48-h treatment, coverslips were fixed and stained for the double-staining immunofluorescence p21/Ki67, respectively labelled in red and green. Nuclei were stained with DAPI. Data are representative of different fields per each condition. The cells were photographed under the fluorescence microscopy (Scale bar = 7 μm; magnification = 63 ×).

2.10. Statistical analysis

All data refer to at least three separate experiments. Data in histograms are shown as average ± S.D. Statistical analysis was performed with GraphPad Prism 5.0 software. Bonferroni's multiple comparison test after one-way ANOVA analysis (unpaired, two-tailed) were employed. Significance was considered as follow: ****p < 0.0001; ***p < 0.001; **p < 0.01; *p < 0.05.

3. Results

3.1. Dose-dependent cell toxicity of cell-free Lactiplantibacillus plantarum OC01 supernatant

First, we determined the minimal dose of the cell-free OC01 supernatant that could contrast the malignant phenotype of colorectal cancer (CRC) with no cytotoxicity. Since fibroblasts represent the main stromal normal cellular component of the tumor microenvironment, we first evaluated the potential toxicity of cell-free OC01 supernatant at three different doses, namely 10 μl, 100 μl, and 200 μl, in normal human fibroblasts. Cells were labelled with propidium iodide, which detects necrotic cells, and Cell Tracker Blue, for monitoring functional mitochondrial activity (i.e., healthy cells). Human fibroblasts showed a dose dependent reduction in cell viability. The highest dose of cell-free OC01 supernatant (200 μl) induced cell death as early as 24 h-treatment, demonstrated by the increase of propidium iodide positive necrotic cells. The toxicity of this dose was further confirmed by the decreased intensity of Cell Tracker fluorescence (data not shown).

Next, we tested the toxicity of cell-free OC01 supernatant in two human CRC, HCT116 and HT29 cells, representative of CRC with different alterations in the main oncogenes and tumor suppressor genes. Essentially, focusing on the driver mutations of CRC, HCT116 cells express wild-type *TP53* and *APC* (Adenomatous Polyposis Coli gene), and mutated *KRAS* and *CTNNB1* (β-Catenin gene), while HT29 cells express mutated *TP53* and *APC*, and wild-type *KRAS*, while no alterations in β-Catenin sequence are reported in this cell line.

The cells were exposed for 72 h to 10 μl and 100 μl of OC01, which were not toxic for normal fibroblasts. Data showed no significant differences in cell viability, demonstrated by the propidium iodide and Cell Tracker, indicating no toxicity (data not shown).

3.2. Cell-free OC01 supernatant suppresses colorectal cancer cell growth

In agreement with previous results, cell counting of viable fibroblasts and CRC cells exposed to 10 μl and 100 μl doses of OC01 showed that cell death was negligible while strongly inhibiting cell proliferation. We observed that 100 μl of cell-free OC01 supernatant decreased the proliferation of both fibroblasts and CRC cells (data not shown), whereas 10 μl reduced the proliferation only in HCT116 and HT29 cell lines (Fig. 1A) without affecting fibroblast cell growth (data not shown). Thus, the latter concentration was chosen for the following experiments.

The flow cytometric analysis revealed that the proportion of HCT116 and HT29 cells in G0/G1phase increased on exposure to cell-free OC01 supernatant, while that in the S and G2/M phases decreased, suggesting a slow transition in cell cycle phases (Fig. 1B).

These data were supported by the immunofluorescence assay for the proliferation markers. The double-staining showed that the exposure to 10 μl of cell-free OC01 supernatant both in HCT116 and HT29 cell lines reduced the expression of Ki67, a proliferative nuclear marker, while it promoted the expression of $p21^{waf/Cip1}$, the cyclin-dependent kinase inhibitor that prevents entering the S phase of the cell cycle (Fig. 1C).

3.3. Cell-free OC01 supernatant limits CRC spheroid growth suppressing the stimulatory effect of IL-6

To evaluate cancer proliferation in a culture system that better recapitulates the *in vivo* structure of the tumor, we tested the efficacy of the cell-free OC01 supernatant by monitoring the growth for up 7 days in a 3D-spheroid forming assay. To partially mimic the inflammatory tumor microenvironment of CRC,[13] we treated the spheroids with IL-6 (one of the most abundant cytokines released by cancer-associated fibroblasts), in the presence or not of probiotic metabolites. The growth of spheroids increased progressively when cultivated in the presence of IL-6. The presence of the probiotic metabolites in the culture medium strongly impaired the 3D tumor growth, as indicated by the fact that the dimension of spheroids remained essentially constant during the incubation time. Worthy of note, the 3D growth-inhibitory effect of the probiotic metabolites was observed also when the cells were challenged with IL-6 (Fig. 2).

Based on DiD staining (whose fluorescence decays proportionally with cell division) of CRC cells grown as 3D spheroids, at day 7 IL-6-treated cells exhibited an elevated proliferative rate, as indicated by the low fluorescence retention compared to time 0h. In contrast, in the presence of probiotic cell-free supernatant, the cells presented a higher retention of DiD fluorescent signal, indicating that cell-free OC01 supernatant metabolites impaired cell duplication even when the cytokine was added to the treatment (Fig. 3A).

These data were further corroborated by the immunofluorescence of $p21^{waf/Cip1}$, whose expression was remarkably reduced in the presence of IL-6 (consistent with increased cell proliferation) and enhanced in the presence of *L. plantarum* OC01 cell-free supernatant (consistent with the decreased cell proliferation) (Fig. 3B).

3.4. Cell-free OC01 supernatant metabolites down-regulate the growth signaling pathway

Abnormal activation of protein kinases downstream the growth factor receptor pathways leads to uncontrolled cell proliferation.[23,24] Likewise, growth factors and nutrients stimulate the activation of the mTOR kinase, which triggers the downstream pathways for protein synthesis and cell growth associated with cell proliferation,[25] while inhibiting autophagy, a macromolecular degradation pathway.[26]

We investigated the modulation of proliferative and survival pathways in CRC spheroids collected at day 7 assessing by Western blotting the phosphorylation of ERK1/2 (that activates mTOR) and of the S6 ribosomal protein, which is phosphorylated by the p70S6

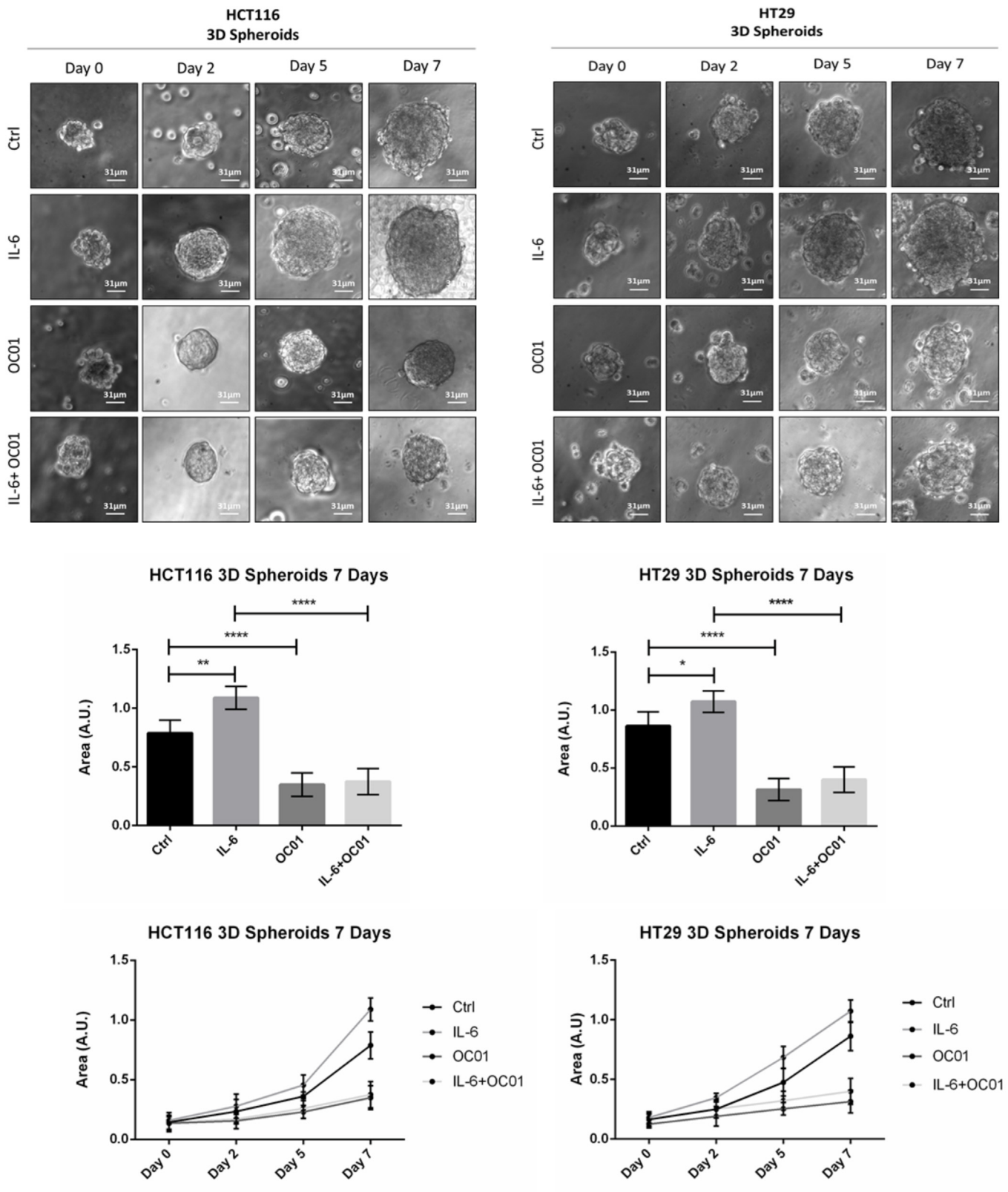

Fig. 2. Cell-free OC01 supernatant reduces 3D-spheroid growth of CRC, also in the presence of the inflammatory cytokine IL-6. HCT116 and HT29 cell line were seeded in poly-HEMA-coated Petri dishes. Cell-free OC01 supernatant and 50 ng/ml IL-6, alone or in combination, were added to culture medium. Medium and treatments were readded every 48 h. The growth of spheroids was monitored by taking pictures at phase contrast microscope up to 7 days of treatment. Data are representative of different fields per each condition. The graph represents the average ± SD (significance was considered as follow: ****$p < 0.0001$; **$p < 0.01$; *$p < 0.05$). Growth curve representing the 3D spheroid dimensions of HCT116 and HT29 during the experimental timeline.

A

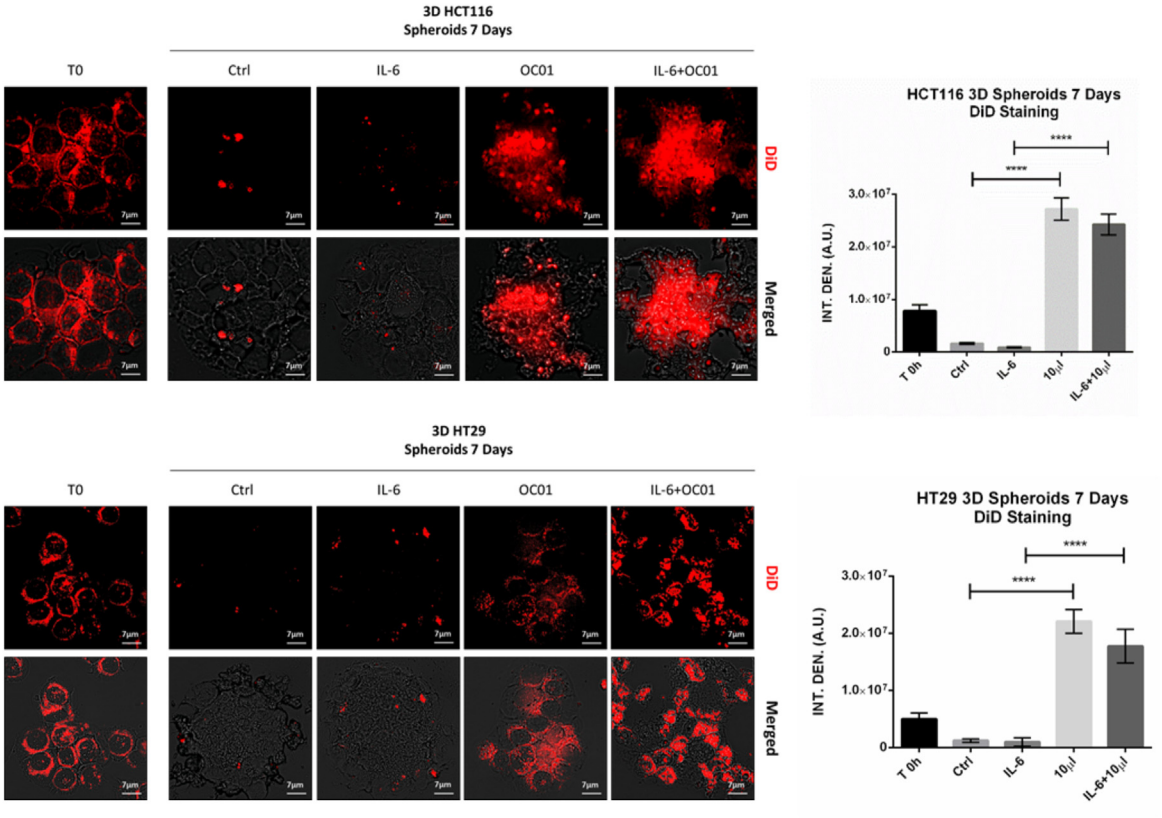
3D HCT116
Spheroids 7 Days
T0
Ctrl
IL-6
OC01
IL-6+OC01
DiD
Merged
7µm
HCT116 3D Spheroids 7 Days
DiD Staining
INT. DEN. (A.U.)
3.0×10⁷
2.0×10⁷
1.0×10⁷
0
****
T 0h
Ctrl
IL-6
10µl
IL-6+10µl
3D HT29
Spheroids 7 Days
HT29 3D Spheroids 7 Days
DiD Staining

B

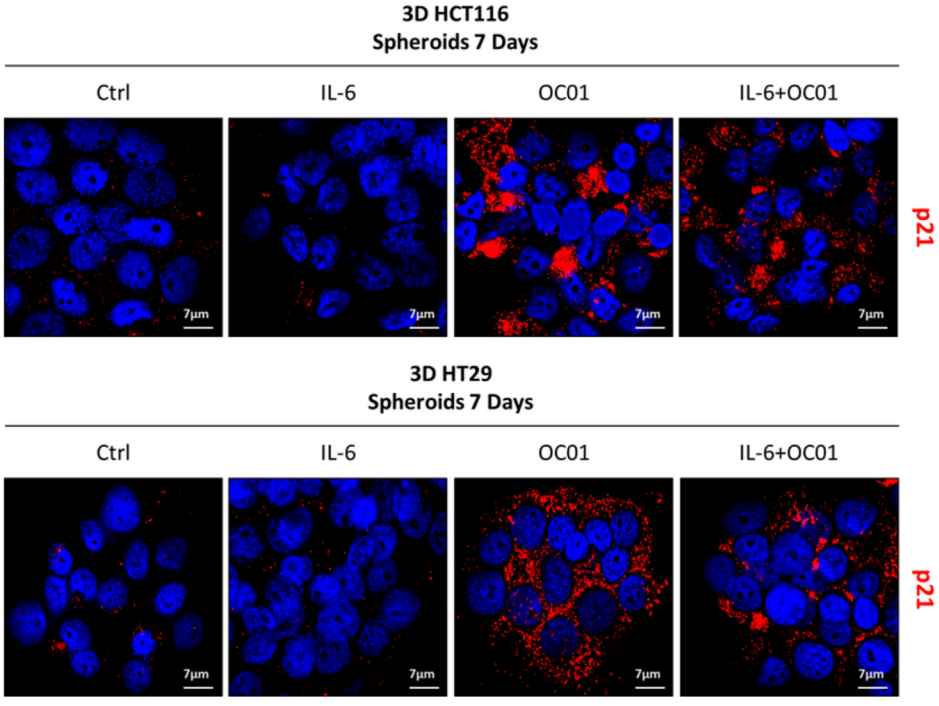
3D HCT116
Spheroids 7 Days
Ctrl
IL-6
OC01
IL-6+OC01
p21
7µm
3D HT29
Spheroids 7 Days

kinase that is downstream of and used as indirect readout of mTOR and ERK1/2 activities.[27] Consistent with the exponential growth of the spheroids (Fig. 2), in control cells, and even more in IL-6 treated cells, both the ERK and mTOR pathways were active as indicated by ERK1/2 and S6 phosphorylation (Fig. 4). Notably, even when under IL-6 stimulation, the supplementation of the OC01 cell-free supernatant to the culture medium reduced the activation of ERK in both the cell lines and decreased the phosphorylation and the expression of the S6 ribosomal protein (downstream to mTOR-p70S6k) respectively in HCT116 cells and in HT29 cells (Fig. 4).

3.5. Cell-free OC01 supernatant suppresses IL-6-induced epithelial to mesenchymal transition and transwell invasion of CRC cells

Finally, we tested the ability of cell-free OC01 supernatant to inhibit cell migration and invasion of CRC cells. First, we performed a classical wound healing scratch assay on HCT116 and HT29 cells and monitored the rate of healing over a 72-h period. HCT116 cells showed an increased cell motility compared to HT29 cells as indicated by the faster closure of the wound. IL-6 greatly stimulated cell migration as shown by the progressive fast closure of the wound, markedly visible at 48 h and causing the nearly complete closure by 72 h, with a rate of healing of 90% in HCT116 and 84% in HT29. In contrast, the migration rate calculated at 72 h was around 34% and 22% for HCT116 and HT29, respectively, when cultivated in the presence of the cell-free OC01 supernatant. The supernatant could slow down CRC cell migration also in the presence of IL-6. In this condition, we appreciated a reduction of healing rate approximately greater than 50% compared to IL-6 alone in both cell lines (Fig. 5A). As these effects could also be ascribed to changes in the proliferation rate, we further investigated how IL-6 and the OC01 supernatant could affect the migratory behavior and phenotype of the cells.

During migration and invasion, cancer cells undergo the so-called epithelial to mesenchymal transition (EMT) characterized by the switch in the expression of the adhesion membrane cadherin from Epithelial-like (E) to Neural-like (N), which is fundamental for avoiding anoikis within the fluid environment. Thus, we checked for the expression of EMT markers performing the immunofluorescence staining of N-Cadherin (marker of metastatic cells) and *E*-Cadherin (marker of non-metastatic cells) in the cells at the migration front. Cell-free OC01 supernatant reduced the expression of N-Cadherin, whereas increased that of *E*-Cadherin, crucial for the maintenance of the epithelial phenotype, in both cell lines. This effect was observed also in the cells stimulated with the inflammatory IL-6 (Fig. 5B).

To definitively rule out that the proliferative capacity of cancer cells in the different experimental conditions could distort the data shown in Fig. 5A, we performed a transwell migratory assay, testing the cellular capability to migrate through the permeable filter. The panel reported in Fig. 5C showing the migrated cells confirms the inhibitory effect of OC01 supernatant on cell locomotion also in the presence of IL-6, in agreement with the wound healing results.

3.6. Butyrate induces autophagy and β-Catenin degradation in HCT116 spheroids

We have previously shown that autophagy contrasts cell migration and cell proliferation.[22,28] We therefore checked whether OC01 supernatant supplementation modulates autophagy. For this experiment we chose HCT116 cells that showed a more malignant phenotype in terms of cell proliferation and migration compared to HT29. The induction of autophagy was investigated by the immunofluorescence double-staining for LC3 (autophagosome marker) and LAMP1 (lysosome marker). As shown in Fig. 6A, OC01 supernatant increased the number of LC3-positive vacuoles interacting with LAMP1 (yellow signal), while IL-6 reduced it. The co-localization of the two proteins in the presence of cell-free OC01 supernatant (yellow signal) was indicative of autophagy induction (Fig. 6A).

The constitutive activation of the WNT/β-Catenin pathway is considered a driver event in colorectal carcinogenesis.[29] As a result, the key effector β-Catenin translocates to the nucleus promoting the expression of target genes involved in cell cycle progression and in cell motility. In a recent study, we found that in CRC cells the β-Catenin gene (*CTNNB1*) positively correlates with several genes regulating the cell cycle and mitosis, cell migration, and epithelial to mesenchymal transition, among others, while it negatively correlates with genes regulating the autophagy-lysosomal pathway.[28] Moreover, we demonstrated that butyrate counteracted cell proliferation through autophagy degradation of β-Catenin in cells defective in the proteasomal degradation of this protein28.

Since butyrate is a component of cell-free *Lactiplantibacillus plantarum* OC01 (NCIMB 30624) supernatant, we tested whether butyrate could induce autophagy and reduce the level of β-Catenin also in the presence of the inflammatory cytokine IL-6. We used the HCT116 cells, which showed the highest 3D spheroid growth and migration rate. As shown in Fig. 6B, IL-6 caused an increased accumulation of β-Catenin along with a block of autophagosome formation (as indicated by the accumulation of LC3-I that was not converted into the autophagosomal associated LC3-II). In contrast, the presence of butyrate in culture conditions caused a drastic reduction of free β-Catenin and stimulated the autophagy degradative pathway (as indicated by the decreased level of LC3-I and increased level of LC3-II) (Fig. 6B).

4. Discussion

Gut microbiota has been found to play a crucial role in cancer development.[30,31] Human gut microbiota is constituted by several microorganisms populating the intestinal mucosa. This complex ecosystem influences host energy metabolism, immune homeostasis, and the maintenance of mucosa integrity. In addition, commensal bacteria compete with pathogens for nutrients and niche colonization, and, from the metabolism of fiber fermentation, they produce the short chain fatty acids (SCFAs) as end products. Among them, butyrate is employed as energy fuel by colonocytes and is involved in the differentiation and proliferation of intestinal cells.[32]

Intestinal barrier breakdown leads to microbiota dysbiosis, characterized by loss of biodiversity in bacterial species, an exacerbated inflammatory response, and epithelial damage in susceptible individuals exposed to environmental risk factors.[30] It is widely reported that gut dysbiosis is related to several diseases, including colorectal cancer.[33] Restoring the correct modulation of the intestinal ecosystem with the supplementation of probiotics

Fig. 3. Cell-free OC01 supernatant reduces the 3D-spheroids proliferation of CRC. HCT116 and HT29 spheroids were cultured and treated as previously described. Data are representative of different fields per each condition. **A)** Cell lines were stained with 1 μM DiD. The intensity of DiD retention was acquired at the fluorescence microscope at time 0 and after 7 day-treatment and quantified with the software ImageJ. The cells were photographed under the fluorescence microscopy (Scale bar = 7 μm; magnification = 63 ×). The graph represents the average ± SD (significance was considered as follow: ****p < 0.0001). **B)** After 7 day-treatment, spheroids were stained for the marker p21 (red). Nuclei were stained with DAPI. The images were acquired at the fluorescence microscope (Scale bar = 7 μm; magnification = 63 ×). The cells were photographed under the fluorescence microscopy.

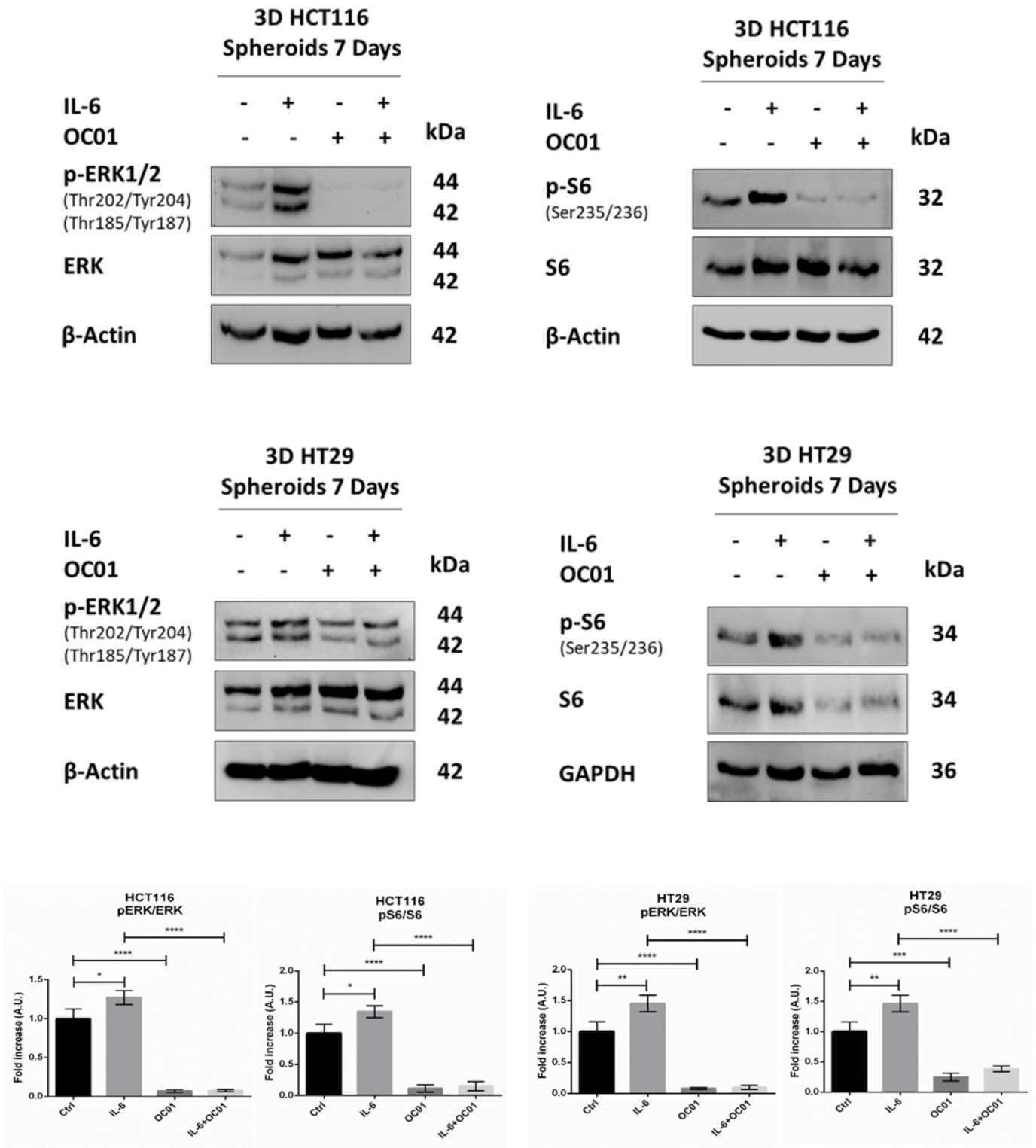

Fig. 4. Cell-free OC01 supernatant reduces the activation of survival molecular pathways in CRC cell lines. Cell-free OC01 supernatant and 50 ng/ml IL-6, alone or in combination, were added to culture medium for 7-day treatment. Spheroid homogenates were processed by using Western blotting to analyze the expression of: pERK1/2 (Thr202/Tyr204-Thr185/Tyr187) and ERK; pS6 (Ser235/236) and S6. The filter was re-probed with β-Actin and GAPDH as loading control. The blots shown in the panels are representative of three experiments. Densitometric data with standard deviation of three separate experiments are included (significance was considered as follow: ****$p < 0.0001$; ***$p < 0.001$; **$p < 0.01$; *$p < 0.05$).

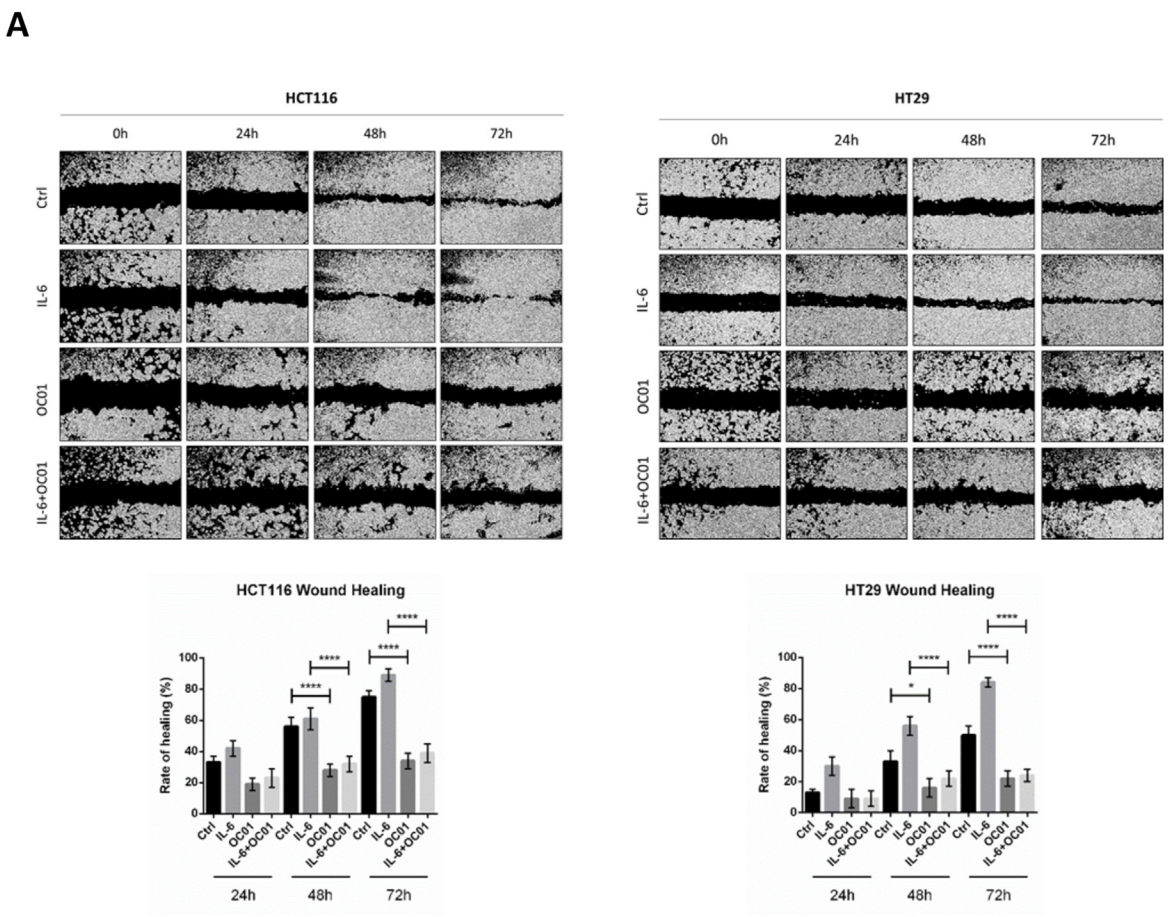

Fig. 5. Cell-free OC01 supernatant counteracts CRC cell migration, also in the presence of IL-6. Cells were seeded in Petri dishes and treated with cell-free OC01 supernatant and 50 ng/ml IL-6, alone or in combination. Medium and treatments were renewed everyday **A)** Cell monolayers were scratched to produce a straight line. The wound closure was monitored up to 72 h by using a phase-contrast microscope. The graph reporting the rate of healing (%) for each experimental time-point was created using ImageJ software. Data represent the average ± SD calculated for three different fields per each condition (significance was considered as follow: ****p < 0.0001; *p < 0.05). **B)** Following 48 h of incubation, coverslips were fixed and stained for N-Cadherin (red) and *E*-Cadherin (green). Nuclei were stained with DAPI. The cells were photographed under the fluorescence microscopy (Scale bar = 7 μm; magnification = 63 ×). Data are representative of different fields per each condition. **C)** After 48 h of culture, cells were collected and placed in the inserts. The migrated cells were photographed in random fields at bright-field microscope (significance was considered as follow: ****p < 0.0001; ***p < 0.001).

that enrich the microbic flora and reduce intestinal inflammation may be a promising strategy to counteract colorectal cancer (CRC) progression.

Probiotics, mainly *Lactobacillus* or *Bifidobacterium* genus, are currently used in the maintenance of health and alleviation of disease symptoms, especially in the gastrointestinal disorders.[34] Moreover, recent studies have described the role of host microbiome in cancer initiation and progression as well as in the modulation of therapeutic responses, improving the outcomes of chemo-and immunotherapy protocols in cancer patients.[35]

Motivated by their promising role in stimulating the growth and the activity of the advantageous bacteria, preventing infections, and moderating the side effects of cancer treatments,[17] we tested the cell-free supernatant of *Lactiplantibacillus plantarum* OC01 (NCIMB 30624) on two colorectal cancer models, HCT116 and HT29. Several studies reported the beneficial anticancer effects of different strains of *L. plantarum* in mouse models. Particularly, the supplementation of this probiotic strain ameliorated the inflammation and colon cancer development in miceh.[36] Moreover, the bacterium could counteract the growth of pathogen bacteria and reduce the expression of inflammatory cytokines associated to pathogen invasion.[37] *L. plantarum* is reported also to decrease the growth and the size of tumor mass *in vivo* experiments.[38]

In the present work, we investigated the effect of the collective bacterial metabolites in the proliferative and migratory features of colorectal cancer cell lines induced by IL-6, a pro-inflammatory cytokine driving the malignant phenotype of tumor and stromal cells and found abundantly secreted in the tumor microenvironment.[22,39] IL-6 is highly released in the serum of CRC-affected patients,[15] and this correlates with increased tumor growth and aggressiveness, and poor clinical outcome.[13,14]

Several studies report the anti-proliferative effects of probiotics in cancer progression.[36,40,41] Here, we found that the cell-free supernatant of *L. plantarum* OC01 has the ability to limit cell proliferation, and, of clinical relevance, this anti-tumor effect was elicited also in the presence of the inflammatory cytokine IL-6. The increased expression of the cyclin-dependent kinase inhibitor p21 is observed when cells are incubated with the OC01 metabolites. Of note, the transcription of p21 is under control of the tumor suppressor gene *TP53*. HCT116 cells present a wild-type *TP53*, thus one possible mechanism of action of the cell-free supernatant OC01 may be the phosphorylation and activation of *TP53*, and thus the promotion of p21 transcription. On the other hand, HT29 cells bear a hotspot mutation in *TP53* (R273H) that results in a loss of DNA

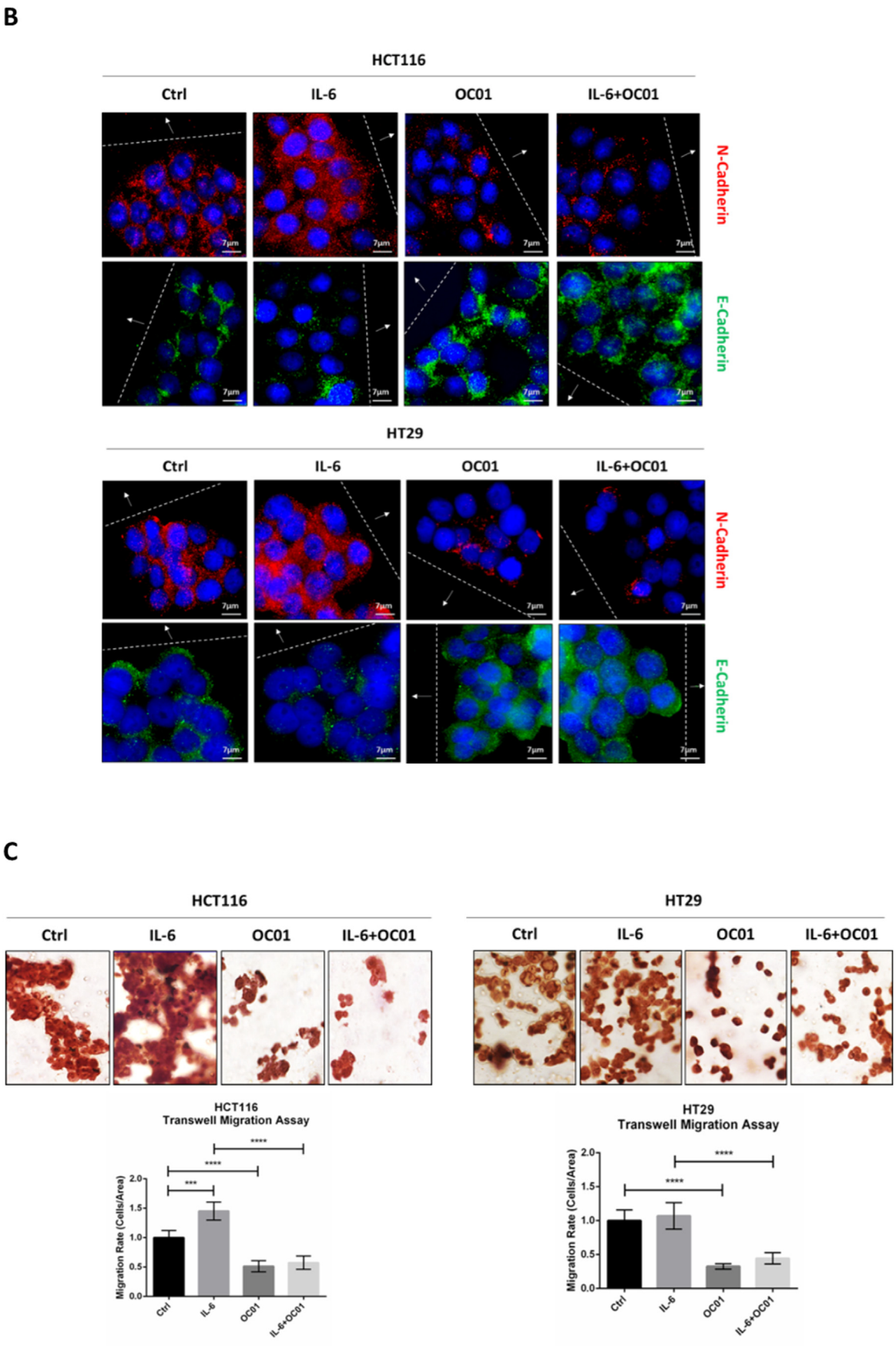

Fig. 5. (*continued*).

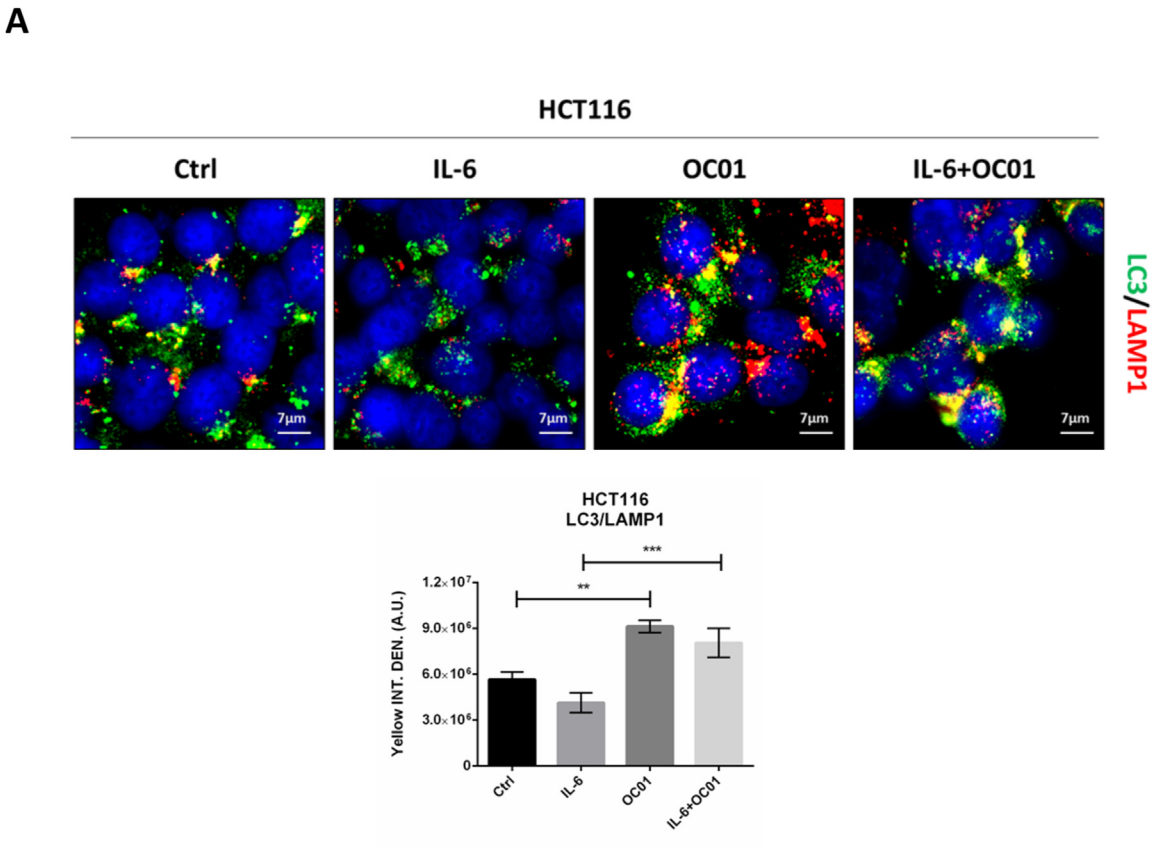
A
HCT116
Ctrl
IL-6
OC01
IL-6+OC01
LC3/LAMP1
7μm
HCT116
LC3/LAMP1
Yellow INT. DEN. (A.U.)
1.2×10⁷
9.0×10⁶
6.0×10⁶
3.0×10⁶
0
**
***
Ctrl
IL-6
OC01
IL-6+OC01

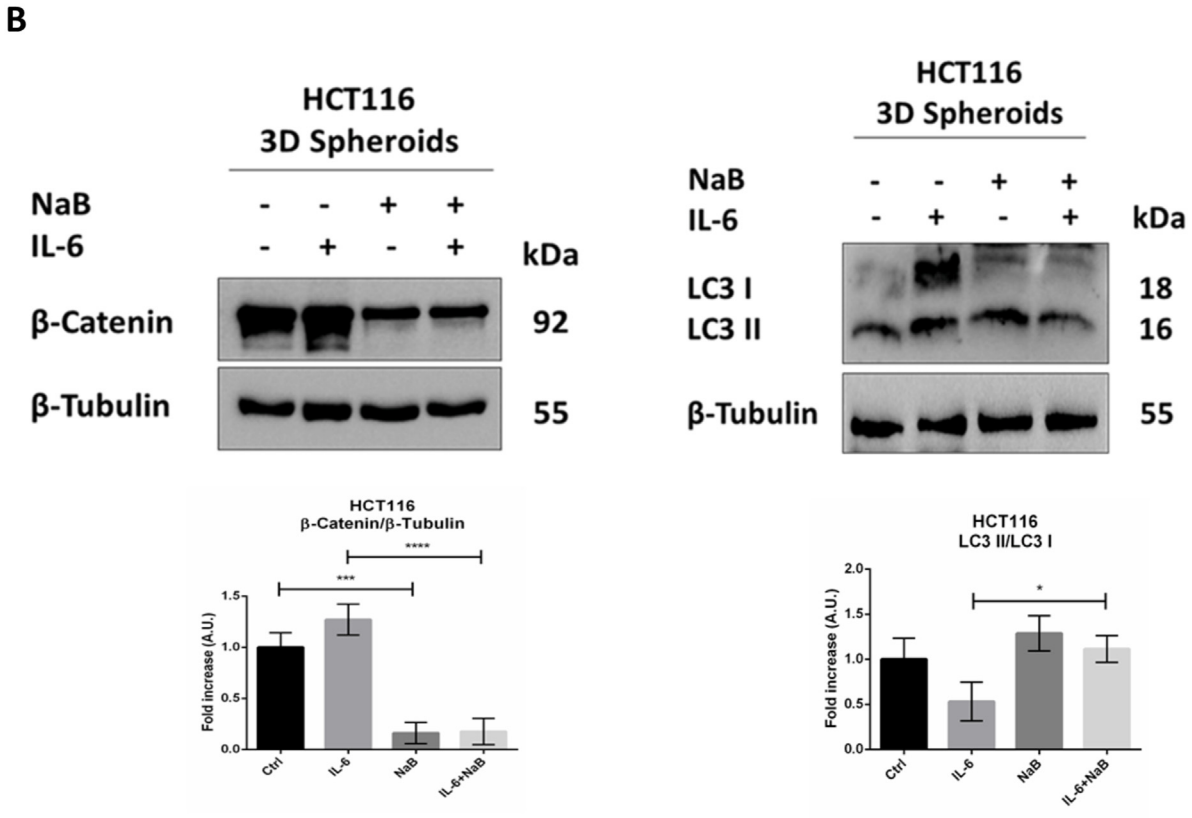
B
HCT116
3D Spheroids
NaB
IL-6
kDa
β-Catenin
92
β-Tubulin
55
HCT116
β-Catenin/β-Tubulin
Fold increase (A.U.)
Ctrl
IL-6
NaB
IL-6+NaB
HCT116
3D Spheroids
NaB
IL-6
kDa
LC3 I
LC3 II
18
16
β-Tubulin
55
HCT116
LC3 II/LC3 I
Fold increase (A.U.)
Ctrl
IL-6
NaB
IL-6+NaB

Fig. 6. Probiotic metabolites reduce β-Catenin level and promotes autophagy. HCT116 were treated with NaB or cell-free OC01 supernatant in the presence or absence of 50 ng/ml IL-6. **A)** Coverslips were fixed and stained for LC3 (green) and LAMP1 (red). Nuclei were stained with DAPI. The cells were photographed under the fluorescence microscopy (Scale bar = 7 μm; magnification = 63 ×). Data are representative of different fields per each condition. Data are from their different images for each condition. The graph represents the integrity density ± SD (significance was considered as follow: ***p < 0.001; **p < 0.01). **B**) Spheroid homogenates were processed by Western blotting to evaluate the expression of β-Catenin and LC3. The filter was reprobed with β-Tubulin as loading control. Densitometric analysis are included (significance was considered as follow: ****p < 0.0001; ***p < 0.001; *p < 0.05).

binding and altered transcription of the tumor suppressor target genes, leading to the failure of cell cycle arrest.[42,43] Yet, it has been reported that some TP53 mutants, among which the R273H, may retain the ability to transactivate the promoter of p21.[44] Definitely, the pathway of p21 induction by the OC01 supernatant deserves further investigations.

Several genetic and epigenetic alterations in genes encoding for growth factor receptors, molecules of signaling network (e.g., Ras, Raf, mTOR) or cell cycle regulatory proteins (e.g., p21, p53) lead to uncontrolled cell proliferation.[45,46] Current therapy is based on neoplastic chemotherapy or targeted therapy with monoclonal antibodies or peptides targeting VEGF or EGFR.[7,8] However, drug resistance is one of the main issues in cancer management. Here, we demonstrated that the supplementation of the probiotic supernatant OC01 modulated oncogenic pathways downstream to these receptors/growth factors, typical targets of the neoplastic treatment and target therapy. In particular, ERK kinases indirectly enhances mTOR activity (through inhibition of TSC1), which directs protein synthesis (through activation of p70S6K) and cell mass accumulation required for progressing in the cell cycle.[47] These signaling pathways are triggered by the activation of Ras, and consistently the employment of current monoclonal antibodies *anti*-EGFR are effective only in tumor bearing a non-mutated *Ras*. The metabolites of *L. plantarum* OC01 that we employed in the present study exceeded these limitations showing a negative modulation in ERK and S6 activation both in HCT116 (mutated *Ras*) and HT29 (wild-type *Ras*). It is likely that other pathways are also involved. In fact, it has been reported that S6 could be phosphorylated on S235 and S236 via Ras-Raf-MEK-ERK also when the mTOR-p70S6K pathway was inhibited.[48] Thus, we cannot exclude an mTOR-independent action of the probiotic metabolite on S6, for instance through a direct action on p70S6K. Intriguingly, in HT29 cells, which are *TP53* and *APC* mutated, the OC01 probiotic supernatant caused a drastic reduction of S6 protein level, likely due to degradation.

Cell migration is a hallmark of cancer cells. In cancer progression, cancer cells undergo epithelial to mesenchymal transition (EMT) and acquire a mesenchymal phenotype.[49] During the transition, epithelial cells lose their junctions and apical-basal polarity, reorganize the cytoskeleton, reprogram gene expression, and change shape. This phenotypic reprogramming increases the migratory and invasive capabilities of cells that undergo EMT.[50] We proved the capability of the OC01-derived metabolites to counteract IL-6-induced colorectal cancer cell migration, exerting their anti-migratory effect by down-regulating mesenchymal markers in the cell at the migration front.

The autophagy process is involved in the maintenance of intestinal homeostasis and its deregulation exacerbates the immune system response, leading to chronic inflammation and increasing risk of CRC.[51] Our group recently demonstrated that autophagy contrasts cell proliferation in CRC. Moreover, in CRC patients β-Catenin gene (*CTNNB1*) positively correlates with genes regulating the cell cycle and mitosis, cell migration and EMT, among others, while it negatively correlates with genes regulating the autophagy pathway.[28] Moreover, several studies describe autophagy as the main mechanisms underlying the beneficial effects of probiotics.[52] Consistently, we found that the metabolites of *L. plantarum* OC01 induced autophagy in CRC and that butyrate, a component of the cell-free supernatant, reduced the content of β-Catenin in spheroids exposed to the inflammatory stimulus of IL-6, suggesting its autophagy degradation.

Taken together, this study demonstrated the beneficial properties of probiotics on CRC cancer cell proliferation and migration and provides the pre-clinical rationale for the employment of this probiotic formulation in cancer treatment. A tailored use of probiotics strains producing beneficial metabolites may restore the eubiotic microbiota counteracting the dysbiosis of CRC patients and improving their health status.

Declaration of competing interest

To the best of our knowledge, the named authors have no conflict of interest, financial or otherwise.

Acknowledgements

LV was supported with a PhD fellowship granted by the Italian Ministry of Education, University and Research (MIUR, Rome, Italy) and the Associazione per la Ricerca Medica Ippocrate-Rhazi (ARMIR, Novara, Italy). BG is recipient of a PhD fellowship granted by Comoli, Ferrari & C. SpA (Novara, Italy). The research was partly contributed by unconditional funding from Probiotical SpA (Novara, Italy). The fluorescence microscope was kindly donated by Comoli, Ferrari & C. SpA, Novara (Italy).

References

1. Keku TO, Dulal S, Deveaux A, Jovov B, Han X. The gastrointestinal microbiota and colorectal cancer. *Am J Physiol Gastrointest Liver Physiol*. 2015 Mar 1;308(5):G351–G363. https://doi.org/10.1152/ajpgi.00360.2012. Epub 2014 Dec 24. PMID: 25540232; PMCID: PMC4346754.
2. den Besten G, van Eunen K, Groen AK, Venema K, Reijngoud DJ, Bakker BM. The role of short-chain fatty acids in the interplay between diet, gut microbiota, and host energy metabolism. *J Lipid Res*. 2013 Sep;54(9):2325–2340. https://doi.org/10.1194/jlr.R036012. Epub 2013 Jul 2. PMID: 23821742; PMCID: PMC3735932.
3. Panebianco C, Potenza A, Andriulli A, Pazienza V. Exploring the microbiota to better understand gastrointestinal cancers physiology. *Clin Chem Lab Med*. 2018 Aug 28;56(9):1400–1412. https://doi.org/10.1515/cclm-2017-1163. PMID: 29630505.
4. Petersen C, Round JL. Defining dysbiosis and its influence on host immunity and disease. *Cell Microbiol*. 2014 Jul;16(7):1024–1033. https://doi.org/10.1111/cmi.12308. Epub 2014 Jun 2. PMID: 24798552; PMCID: PMC4143175.
5. Parida S, Sharma D. The microbiome and cancer: creating friendly neighborhoods and removing the foes within. *Cancer Res*. 2021 Feb 15;81(4):790–800. https://doi.org/10.1158/0008-5472.CAN-20-2629. Epub 2020 Nov 4. PMID: 33148661.
6. Zegarra Ruiz DF, Kim DV, Norwood K, et al. Microbiota manipulation to increase macrophage IL-10 improves colitis and limits colitis-associated colorectal cancer. *Gut Microb*. 2022 Jan-Dec;14(1), 2119054. https://doi.org/10.1080/19490976.2022.2119054. PMID: 36062329; PMCID: PMC9450902.
7. Van Cutsem E, Cervantes A, Nordlinger B, Arnold D, ESMO Guidelines Working Group. Metastatic colorectal cancer: ESMO Clinical Practice Guidelines for diagnosis, treatment and follow-up. *Ann Oncol*. 2014 Sep;25(Suppl 3:iii):1–9. https://doi.org/10.1093/annonc/mdu260. . Epub 2014 Sep 4. Erratum in: Ann Oncol. 2015 Sep;26 Suppl 5:v174-v177. PMID: 25190710.
8. Van Cutsem E, Nordlinger B, Cervantes A, ESMO Guidelines Working Group. Advanced colorectal cancer: ESMO clinical practice guidelines for treatment. *Ann Oncol*. 2010 May;21(Suppl 5):v93–v97. https://doi.org/10.1093/annonc/mdq222.PMID:20555112.
9. Longley DB, Allen WL, Johnston PG. Drug resistance, predictive markers and pharmacogenomics in colorectal cancer. *Biochim Biophys Acta*. 2006 Dec;1766(2):184–196. https://doi.org/10.1016/j.bbcan.2006.08.001. Epub 2006 Aug 9. PMID: 16973289.
10. Arnold M, Sierra MS, Laversanne M, Soerjomataram I, Jemal A, Bray F. Global

patterns and trends in colorectal cancer incidence and mortality. *Gut*. 2017 Apr;66(4):683–691. https://doi.org/10.1136/gutjnl-2015-310912. Epub 2016 Jan 27. PMID: 26818619.
11. Wang K, Karin M. Tumor-elicited inflammation and colorectal cancer. *Adv Cancer Res*. 2015;128:173–196. https://doi.org/10.1016/bs.acr.2015.04.014. Epub 2015 May 28. PMID: 26216633.
12. Foran E, Garrity-Park MM, Mureau C, et al. Upregulation of DNA methyltransferase-mediated gene silencing, anchorage-independent growth, and migration of colon cancer cells by interleukin-6. *Mol Cancer Res*. 2010 Apr;8(4):471–481. https://doi.org/10.1158/1541-7786.MCR-09-0496. Epub 2010 Mar 30. PMID: 20354000.
13. Toyoshima Y, Kitamura H, Xiang H, et al. IL6 modulates the immune status of the tumor microenvironment to facilitate metastatic colonization of colorectal cancer cells. *Cancer Immunol Res*. 2019 Dec;7(12):1944–1957. https://doi.org/10.1158/2326-6066.CIR-18-0766. Epub 2019 Sep 25. PMID: 31554639.
14. Waldner MJ, Foersch S, Neurath MF. Interleukin-6–a key regulator of colorectal cancer development. *Int J Biol Sci*. 2012;8(9):1248–1253. https://doi.org/10.7150/ijbs.4614. Epub 2012 Oct 24. PMID: 23136553; PMCID: PMC3491448.
15. Knüpfer H, Preiss R. Serum interleukin-6 levels in colorectal cancer patients–a summary of published results. *Int J Colorectal Dis*. 2010 Feb;25(2):135–140. https://doi.org/10.1007/s00384-009-0818-8. Epub 2009 Nov 7. PMID: 19898853.
16. Privitera G, Rana N, Scaldaferri F, Armuzzi A, Pizarro TT. Novel insights into the interactions between the gut microbiome, inflammasomes, and gasdermins during colorectal cancer. *Front Cell Infect Microbiol*. 2022 Jan 17;11, 806680. https://doi.org/10.3389/fcimb.2021.806680. PMID: 35111698; PMCID: PMC8801609.
17. Molska M, Reguła J. Potential mechanisms of probiotics action in the prevention and treatment of colorectal cancer. *Nutrients*. 2019 Oct 14;11(10):2453. https://doi.org/10.3390/nu11102453. PMID: 31615096; PMCID: PMC6835638.
18. Guiomar de Almeida Brasiel P, Cristina Potente Dutra Luquetti S, Dutra Medeiros J, et al. Kefir modulates gut microbiota and reduces DMH-associated colorectal cancer via regulation of intestinal inflammation in adulthood offsprings programmed by neonatal overfeeding. *Food Res Int*. 2022 Feb;152, 110708. https://doi.org/10.1016/j.foodres.2021.110708. Epub 2021 Sep 8. PMID: 35181109.
19. Zeng X, Jia H, Shi Y, et al. Lactobacillus kefiranofaciens JKSP109 and Saccharomyces cerevisiae JKSP39 isolated from Tibetan kefir grain co-alleviated AOM/DSS induced inflammation and colorectal carcinogenesis. *Food Funct*. 2022 Jul 4;13(13):6947–6961. https://doi.org/10.1039/d1fo02939h. PMID: 35575226.
20. Esposito A, Ferraresi A, Salwa A, Vidoni C, Dhanasekaran DN, Isidoro C. Resveratrol contrasts IL-6 pro-growth effects and promotes autophagy-mediated cancer cell dormancy in 3D ovarian cancer: role of miR-1305 and of its target ARH-I. *Cancers*. 2022 Apr 25;14(9):2142. https://doi.org/10.3390/cancers14092142. PMID: 35565270; PMCID: PMC9101105.
21. Ferraresi A, Esposito A, Girone C, et al. Resveratrol contrasts LPA-induced ovarian cancer cell migration and platinum resistance by rescuing hedgehog-mediated autophagy. *Cells*. 2021 Nov 17;10(11):3213. https://doi.org/10.3390/cells10113213. PMID: 34831435; PMCID: PMC8625920.
22. Ferraresi A, Phadngam S, Morani F, et al. Resveratrol inhibits IL-6-induced ovarian cancer cell migration through epigenetic up-regulation of autophagy. *Mol Carcinog*. 2017 Mar;56(3):1164–1181. https://doi.org/10.1002/mc.22582. Epub 2016 Nov 3. PMID: 27787915.
23. Degirmenci U, Wang M, Hu J. Targeting aberrant RAS/RAF/MEK/ERK signaling for cancer therapy. *Cells*. 2020 Jan 13;9(1):198. https://doi.org/10.3390/cells9010198. PMID: 31941155; PMCID: PMC7017232.
24. Mirza-Aghazadeh-Attari M, Ekrami EM, Aghdas SAM, et al. Targeting PI3K/Akt/mTOR signaling pathway by polyphenols: implication for cancer therapy. *Life Sci*. 2020 Aug 15;255, 117481. https://doi.org/10.1016/j.lfs.2020.117481. Epub 2020 Mar 2. PMID: 32135183.
25. Cargnello M, Tcherkezian J, Roux PP. The expanding role of mTOR in cancer cell growth and proliferation. *Mutagenesis*. 2015 Mar;30(2):169–176. https://doi.org/10.1093/mutage/geu045. PMID: 25688110; PMCID: PMC5943824.
26. Giguère V. Canonical signaling and nuclear activity of mTOR-a teamwork effort to regulate metabolism and cell growth. *FEBS J*. 2018 May;285(9):1572–1588. https://doi.org/10.1111/febs.14384. Epub 2018 Jan 31. PMID: 29337437.
27. Laplante M, Sabatini DM. mTOR signaling in growth control and disease. *Cell*. 2012 Apr 13;149(2):274–293. https://doi.org/10.1016/j.cell.2012.03.017. PMID: 22500797; PMCID: PMC3331679.
28. Garavaglia B, Vallino L, Ferraresi A, et al. Butyrate inhibits colorectal cancer cell proliferation through autophagy degradation of β-catenin regardless of APC and β-catenin mutational status. *Biomedicines*. 2022 May 13;10(5):1131. https://doi.org/10.3390/biomedicines10051131. PMID: 35625868; PMCID: PMC9138675.
29. Bian J, Dannappel M, Wan C, Firestein R. Transcriptional regulation of wnt/β-catenin pathway in colorectal cancer. *Cells*. 2020 Sep 19;9(9):2125. https://doi.org/10.3390/cells9092125. PMID: 32961708; PMCID: PMC7564852.
30. Song M, Chan AT. Environmental factors, gut microbiota, and colorectal cancer prevention. *Clin Gastroenterol Hepatol*. 2019;17(2):275–289. https://doi.org/10.1016/j.cgh.2018.07.012.
31. Roy S, Trinchieri G. Microbiota: a key orchestrator of cancer therapy. *Nat Rev Cancer*. 2017;17(5):271–285. https://doi.org/10.1038/nrc.2017.13.
32. Song M, Chan AT, Sun J. Influence of the gut microbiome, diet, and environment on risk of colorectal cancer. *Gastroenterology*. 2020 Jan;158(2):322–340. https://doi.org/10.1053/j.gastro.2019.06.048. Epub 2019 Oct 3. PMID: 31586566; PMCID: PMC6957737.
33. Gomaa EZ. Human gut microbiota/microbiome in health and diseases: a review. *Antonie Leeuwenhoek*. 2020 Dec;113(12):2019–2040. https://doi.org/10.1007/s10482-020-01474-7. Epub 2020 Nov 2. PMID: 33136284.
34. Plaza-Diaz J, Ruiz-Ojeda FJ, Gil-Campos M, Gil A. Mechanisms of action of probiotics. *Adv Nutr*. 2019 Jan 1;10(suppl_1):S49–S66. https://doi.org/10.1093/advances/nmy063. Erratum in: Adv Nutr. 2020 Jul 1;11(4):1054. PMID: 30721959; PMCID: PMC6363529.
35. Panebianco C, Latiano T, Pazienza V. Microbiota manipulation by probiotics administration as emerging tool in cancer prevention and therapy. *Front Oncol*. 2020 May 22;10:679. https://doi.org/10.3389/fonc.2020.00679. PMID: 32523887; PMCID: PMC7261958.
36. Ma F, Sun M, Song Y, et al. Lactiplantibacillus plantarum-12 alleviates inflammation and colon cancer symptoms in AOM/DSS-Treated mice through modulating the intestinal microbiome and metabolome. *Nutrients*. 2022 May 3;14(9):1916. https://doi.org/10.3390/nu14091916. PMID: 35565884; PMCID: PMC9100115.
37. Wang Y, Li J, Ma C, et al. Lactiplantibacillus plantarum HNU082 inhibited the growth of Fusobacterium nucleatum and alleviated the inflammatory response introduced by F. nucleatum invasion. *Food Funct*. 2021 Nov 1;12(21):10728–10740. https://doi.org/10.1039/d1fo01388b.PMID:34608480.
38. Fareez IM, Lim SM, Ramasamy K. Chemoprevention by microencapsulated Lactiplantibacillus plantarum LAB12 against orthotopic colorectal cancer mice is associated with apoptosis and anti-angiogenesis. *Probiotics Antimicrob Proteins*. 2022 Dec 12. https://doi.org/10.1007/s12602-022-10020-y. Epub ahead of print. PMID: 36508139.
39. Thongchot S, Ferraresi A, Vidoni C, et al. Resveratrol interrupts the pro-invasive communication between cancer associated fibroblasts and cholangiocarcinoma cells. *Cancer Lett*. 2018 Aug 28;430:160–171. https://doi.org/10.1016/j.canlet.2018.05.031. Epub 2018 May 23. Erratum in: Cancer Lett. 2018 Oct 10;434:206-207. PMID: 29802929.
40. Dikeocha IJ, Al-Kabsi AM, Chiu HT, Alshawsh MA. Faecalibacterium prausnitzii ameliorates colorectal tumorigenesis and suppresses proliferation of HCT116 colorectal cancer cells. *Biomedicines*. 2022 May 13;10(5):1128. https://doi.org/10.3390/biomedicines10051128. PMID: 35625865; PMCID: PMC9138996.
41. Alam Z, Shang X, Effat K, et al. The potential role of prebiotics, probiotics, and synbiotics in adjuvant cancer therapy especially colorectal cancer. *J Food Biochem*. 2022 Oct;46(10), e14302. https://doi.org/10.1111/jfbc.14302. Epub 2022 Jul 11. PMID: 35816322.
42. Freed-Pastor WA, Prives C. Mutant p53: one name, many proteins. *Genes Dev*. 2012 Jun 15;26(12):1268–1286. https://doi.org/10.1101/gad.190678.112. PMID: 22713868; PMCID: PMC3387655.
43. Boettcher S, Miller PG, Sharma R, et al. A dominant-negative effect drives selection of TP53 missense mutations in myeloid malignancies. *Science*. 2019 Aug 9;365(6453):599–604. https://doi.org/10.1126/science.aax3649. PMID: 31395785; PMCID: PMC7327437.
44. Campomenosi P, Monti P, Aprile A, et al. p53 mutants can often transactivate promoters containing a p21 but not Bax or PIG3 responsive elements. *Oncogene*. 2001 Jun 14;20(27):3573–3579. https://doi.org/10.1038/sj.onc.1204468. PMID: 11429705.
45. Roskoski Jr R. Targeting ERK1/2 protein-serine/threonine kinases in human cancers. *Pharmacol Res*. 2019 Apr;142:151–168. https://doi.org/10.1016/j.phrs.2019.01.039. Epub 2019 Feb 20. Erratum in: Pharmacol Res. 2019 May;143:206. PMID: 30794926.
46. Linnskog R, Jönsson G, Axelsson L, Prasad CP, Andersson T. Interleukin-6 drives melanoma cell motility through p38α-MAPK-dependent up-regulation of WNT5A expression. *Mol Oncol*. 2014 Dec;8(8):1365–1378. https://doi.org/10.1016/j.molonc.2014.05.008. Epub 2014 May 27. PMID: 24954857; PMCID: PMC5528610.
47. Ma L, Chen Z, Erdjument-Bromage H, Tempst P, Pandolfi PP. Phosphorylation and functional inactivation of TSC2 by Erk implications for tuberous sclerosis and cancer pathogenesis. *Cell*. 2005 Apr 22;121(2):179–193. https://doi.org/10.1016/j.cell.2005.02.031. PMID: 15851026.
48. Biever A, Valjent E, Puighermanal E. Ribosomal protein S6 phosphorylation in the nervous system: from regulation to function. *Front Mol Neurosci*. 2015 Dec 16;8:75. https://doi.org/10.3389/fnmol.2015.00075. PMID: 26733799; PMCID: PMC4679984.
49. Vu T, Datta PK. Regulation of EMT in colorectal cancer: a culprit in metastasis. *Cancers*. 2017 Dec 16;9(12):171. https://doi.org/10.3390/cancers9120171. PMID: 29258163; PMCID: PMC5742819.
50. Thiery JP, Sleeman JP. Complex networks orchestrate epithelial-mesenchymal transitions. *Nat Rev Mol Cell Biol*. 2006 Feb;7(2):131–142. https://doi.org/10.1038/nrm1835. PMID: 16493418.
51. Yang L, Liu C, Zhao W, et al. Impaired autophagy in intestinal epithelial cells alters gut microbiota and host immune responses. *Appl Environ Microbiol*. 2018 Aug 31;84(18):18. https://doi.org/10.1128/AEM.00880-18. PMID: 30006408; PMCID: PMC6121970 e00880.
52. Nemati M, Omrani GR, Ebrahimi B, Montazeri-Najafabady N. The beneficial effects of probiotics via autophagy: a systematic review. *BioMed Res Int*. 2021 Dec 3, 2931580. https://doi.org/10.1155/2021/2931580. PMID: 34901266; PMCID: PMC8664546 2021.